Journal of Intelligent Systems and Control
https://www.acadlore.com/journals/JISC

Design of an Optimized Robust Deadbeat Controller for Roll Motion in Tail-Sitter VTOL UAVs

Ali H. Mhmood

Petroleum Systems Control Engineering Department, College of Petroleum Processes Engineering, Tikrit University, 34001 Tikrit, Iraq

* Correspondence: Ali H. Mhmood (ali.h.mhmood@tu.edu.iq)

Received: 02-04-2024 **Revised:** 03-13-2024 **Accepted:** 03-22-2024

Citation: A. H. Mhmood, "Design of an optimized robust deadbeat controller for roll motion in tail-sitter VTOL UAVs," *J. Intell Syst. Control*, vol. 3, no. 1, pp. 21–32, 2024. https://doi.org/10.56578/jisc030102.

Abstract: Unmanned Aerial Vehicles (UAVs), have recently sparked attention due to its versatility in a wide range of real-life uses. They require to be controlled so as to conduct different operations and widen their typical roles. This study proposes an optimal robust deadbeat controller for the roll angle motion of tail-sitter vertically take-off and land vehicles, taking into consideration the systems' intrinsic sensitivity to outside influences and fluctuation of their dynamics. Primarily, several assumptions are used to develop an appropriate transfer function that reflects the system physical attributes. The suggested controller is then formed in two sections: the first section addresses the nominal system's unstable dynamics, and the second element imposes the desired deadbeat performance and robustness. The control system variables are optimized using the creative and efficient Incomprehensible but Time-Intelligible Logics optimization technique, ensuring that the specified robustness demand is satisfied correctly. Finally, simulation is used to evaluate the developed controller effectiveness, revealing beneficial stability and performance indicators for both nominal and uncertain regulated system featuring uniform, bounded, and feasible closed-loop outputs. The control unit performs well, with a rising time of 0.0965 seconds, a settling time of 0.1134 seconds, and an overshoot of 0.167%.

Keywords: Robust control; Deadbeat control; Roll angle; Tail-sitter; VTOL vehicle; UAV; Incomprehensible but Time-Intelligible Logics optimization

1 Introduction

Unmanned Aerial Vehicles (UAVs) have lately acquired traction owing to their adaptability in a variety of applications in practice, such as disaster readiness, ecological surveillance, traffic supervision, architectural evaluation, police checks, and military assistance. It is possible to perform several UAV tasks to expand their typical functions, such as increased flying longevity, VTOL systems and floating characteristics. In addition, these small aircraft must be capable of converting from a single setup to a different one, which has lately become critical. Furthermore, coupling the lateral movement attributes of stationary aircraft with the lifting and lowering abilities offered by a chopper can result in prospective UAVs with distinctive dynamic operating features at affordable costs relative to comparable traditional ones. As a result, they need to be controlled in order to perform various tasks, broaden their traditional duties and create platforms that govern dynamical operations, providing transformational applications in a variety of industries. The combination of control engineering and UAV systems has enormous potential to transform industry and address social issues [1–4]. Figure 1 depicts the most straightforward sort of VTOL UAV: A tail-sitter, which takes off and lands on its rear axle before horizontally shifting for flight ahead. This kind is free of further actuation [4, 5].

Different applicable and contemporary control techniques have been proposed to control the flight of the tail-sitter vehicle system. Wang et al. [6] developed a unique arrangement to accommodate the dual rotary tail-sitter. The presented strategy has the potential to provide excellent rejection of disturbances by shortening the gap from elevators to rotors (Figure 1), enhancing the velocity of circulation and resulting in sufficient control thrust required to compensate the aircraft despite wind disturbance [6]. In addition, Garcia-Nieto et al. [7] proposed and executed a technique that controls an autonomous flying wing during a VTOL movement utilizing two shifting rotors, termed a bi-rotor, where the complicated actions associated with the aircraft were analyzed and a strategy to properly

regulate its orientation while hovering was posed. After that, Barth et al. [8] laid out a control strategy that uses a model-independent technique to stabilize the position of tail-sitter mini-aircraft in the presence of wind perturbations throughout four flight treatments: upward launch, forward motion, hovering, and straight drop. Besides, Zhou et al. [9] suggested system identification and model predictive control for a tail-sitter UAV while on a cruise flight. The model was created using least-squares analysis and trust-region techniques, confirmed using outside flying testing, and then utilized for flight simulations [9]. Then, Al-Qassar et al. [2] developed optimal sliding mode control (SMC) and super-twisting sliding mode control (STSMC) for the roll behavior of VTOL UAVs in hovering flight with nonparametric uncertainty. They demonstrated stability evaluation and asymptotic error elimination relying on the Lyapunov theorem. Besides, grey-wolf optimization was used as a tuning method to increase the performance of the control method [2]. In addition, Ajel et al. [3] proposed a Model Reference Adaptive Control (MRAC) method for the UAV system. The adaptive rules were designed for non-parametric uncertainty. A Lyapunov-based stability analysis was performed by considering the uniform ultimate region of the tracking error. The dead-zone adjustment under adaptive laws assured the uniform bounding of all signals, tackling unreasonable drifting in signals and boosting the controller robustness [3]. Moreover, Mhmood and Ali [4] designed an H-infinity model reference Proportion Integration Differentiation (PID) controller for the system at hand, where the black hole optimization method optimizes the controller to ensure that system output synchronously tracks the reference model output, and that any outputs in the associated control system are constrained. Subsequently, Xin et al. [10] developed a control system for a quadrotor tail-sitter UAV, with an emphasis on transitioning between hover and level flight phases. The control system employed a dual-Euler approach, which combines Euler-angle expressions in two body-fixed coordinate sets to offer a continuous attitude description over the flying range. Also, the system was separated into hovering and levelling controllers, with flight level directing using the vector field approach and hover flying using quadrotors [10]. Additionally, Tal and Karaman [11] designed a control rule to control the limber paths of the UAV. The control system has tracked position navigation, velocity, acceleration, jerk, yaw reference, and yaw rate, which improves trajectory tracking with rapidly changing accelerations. Then, the controller performed the control adjustments using incremental nonlinear dynamic inversion (INDI) [11]. Next, Zhong et al. [12] formulated a control system for a miniature tail-sitter vehicle during the transition phase using an L1 neural network adaptive control structure associated with PID control, which enhanced the compensation function and ensured a safe transition. Afterwards, Yang et al. [13] developed a discrete-time linear quadratic regulator (LQR) with an initial deteriorate measure to identify the optimal system pole position, along with a novel angular acceleration estimation method utilized for compensating the unmodelled features.

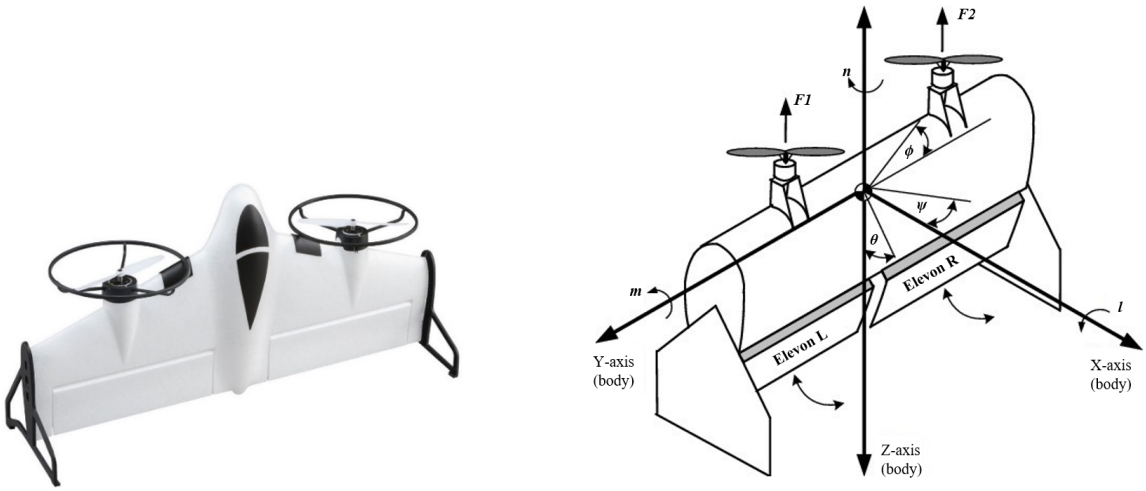

(a) (b)

Figure 1. Experimental tail-sitter VTOL UAV: (a) Realistic arrangement; (b) Operation scheme [5]

Previous research investigations have revealed that the motion patterns of tail-sitters change substantially while flying, prompting the use of robust control to solve this problematic challenge. Additionally, the fundamental nature of such mechanisms, together with the importance associated with the UAV's application, make it important to build a control framework capable of obtaining appropriate performance criteria while preserving the requisite robustness over uncertainty and environmental disturbances. One of the most beneficial solutions is occasionally the so-called deadbeat control technique, which guarantees an exact relaxation of the signal that emerges during a finite, restricted number of testing instances by forcing the closed-loop system to produce a deadbeat reaction that proceeds swiftly

to reach the intended value and remains there without any overshoot [14, 15]. This control method primarily aims to construct a two-part controller structure. The first part cancels the nominal system dynamics by opposing factors in the controller model, while the second part adjusts to the user's preferences to achieve the desired performance. At the same time, the robustness property is carried out by addressing the control problem using the H_∞ concept that is a prominent and important notion in robust control, where it is often necessary to tune the controller parameters to minimize the H_∞ level of the nominal control system (free control system without perturbations) in order to dismiss or shorten the disturbance effect and to compensate for the uncertainty, which may result in inaccurate cancellation of the system dynamics [4, 15]. Lately, proficient optimization approaches have been used to tune the controller parameters in order to optimize the dynamic behavior of the robust deadbeat control, such as particle swarm optimization (PSO) [15]. However, one of the sophisticated and innovative methods that could be applied for this purpose is the IbILO [16], which is a new optimization approach that seeks to comprehend non-logical aspects of human cognition, consisting of three phases: exploration, integration, and exploitation. IbILO provides many advantages over PSO, such as individual monitoring, efficacy in defining optimal solutions, and reduced calculation time [17]. The IbILO method involves a preparatory phase, specifying the settings and iterations for each model. The model is optimized for specific iterations, with final outcomes sent to the next model and incorporated in the second stage. In the first phase of the technique, each working group selects the top experts (the best value of the population) for a specific sector, using their knowledge to improve their fitness in iterations. Three factors are chosen for each expert: the best expert score, the best expert in any group, and the average of experts in the next iteration. The algorithm then integrates all experts (potential candidates) using the information from the current iteration to enhance their expertise value. Then the IbILO focuses on enhancing participant competence by utilizing aggregate expert information, followed by a follow-up refresh, repeated multiple times until termination conditions are met, with the average of past information established [16, 17].

The main contribution of this paper is the design of a robust deadbeat controller to control the roll motion of the tail-sitter UAV system under the effects of system fluctuation and wind disturbance. The controller variables are optimized by a new and advanced IbILO theory such that robust stability and performance conditions are effectively met with desirable and reasonable levels of control and system signals.

2 Modelling of the Tail-Sitter UAV System

This section describes the dynamic modelling of the tail-sitter VTOL UAV. Basic mathematical concepts are frequently used to accurately forecast the behavior of each system element. Subgraph (b) of Figure 1 illustrates the dynamical scheme of the aircraft system in flight mode. The tail-sitter UAV is envisioned as a rigid vehicle traversing over the atmosphere, with forces and loads applied to its body based on expected item attributes. Furthermore, precise control is required during landing and take-off operations, demanding setup to handle roll, pitch, and yaw motions in a confined space [4, 5]. Two preliminary hypotheses are made [2–5]:

Proposition 1: The UAV flies in a confined area of interest, offering validity for using the mathematical formula based on the flat-earth concept; and

Proposition 2: The rotor and elevator masses were both ignored in the analysis. The mathematical representation is formed by assessing the aircraft's attitude in the kinematic standard frame utilizing the three Euler degrees of freedom (yaw, pitch, and roll), which are often used for aeronautical purposes. Hence, the system dynamics are expressed based on the kinematic formulas of Newton as follows [4, 5]:

$$\begin{aligned}
\dot{P}(t) &= \frac{(J_y - J_z)\, QR}{J_x} + \frac{l(t)}{J_x} \\
\dot{Q}(t) &= \frac{(J_z - J_x)\, RP}{J_y} + \frac{m(t)}{J_y} \\
\dot{R}(t) &= \frac{(J_x - J_y)\, PQ}{J_z} + \frac{n(t)}{J_z}
\end{aligned} \tag{1}$$

where, $\begin{bmatrix} P & Q & R \end{bmatrix}^T$ denotes the angular velocity vector of the main frame (X, Y, Z) to rotate relative to the north-east-down (NED) standard frame (x, y, z). Similarly, $\begin{bmatrix} l & m & n \end{bmatrix}^T$ stands for the torque vector that affects the central point of the UAV mass inside the main frame. Moreover, J_x, J_y and J_z denote the diagonally oriented elements of the inertia matrix J [2–5]:

$$J = \begin{bmatrix} J_x & 0 & 0 \\ 0 & J_y & 0 \\ 0 & 0 & J_z \end{bmatrix} \tag{2}$$

To figure out the motion regarding the roll angle, the roll module becomes the primary concern. In this scenario, the pitch and yaw dynamics are supposed to be negligible and regulated by particular controls so that the following condition holds true:

$$Q(t) = R(t) = 0 \tag{3}$$

With this assumption, Figure 2 exhibits the new tail-sitter VTOL UAV setup. Thus, from Eq. (1), the angular behavior that dictates the roll attitude can possibly be articulated according to the following formula [2–5]:

$$\ddot{\phi}(t) = \frac{l(t)}{J_x} \tag{4}$$

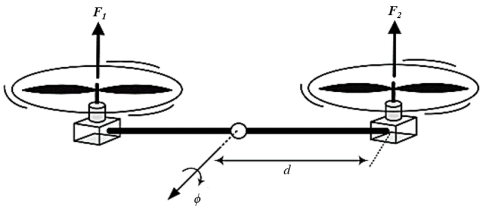

Figure 2. Roll dynamics of the tail-sitter VTOL UAV [3]

where, ϕ refers to the roll angle position. On the other hand, the exerted torque l can be given as follows [2–5]:

$$l(t) = dF(t) - C_l\dot{\phi}(t) \tag{5}$$

where, F is the composite force made up of the difference between the effects of the right and left rotors F_1 and F_2, respectively, indicating the overall thrust exerted on the aircraft mass center, which is characterized as a control signal applied to control the aircraft motion $(F(t) = F_1(t) - F_2(t) = u(t))$. In addition, d refers to the distance between individual rotors and the aircraft's central point, while C_l is a roll damping variation [2–5].

Therefore, applying Eq. (5) to Eq. (1) results in:

$$\ddot{\phi}(t) = -\frac{C_l}{J_x}\dot{\phi}(t) + \frac{d}{J_x}F(t) \tag{6}$$

Next, by setting $\phi(t)$ as the system output and $F(t) = u(t)$ as the control input, the transfer function of the roll angle dynamical motion can be written as [4, 5] :

$$G_U(s) = \frac{\phi(s)}{U(s)} = \frac{d/J_x}{s^2 + (C_l/J_x)\,s} \tag{7}$$

To account for modelling errors, variables d, C_l and J_x are regarded as unknown and given $\pm 10\%$ deviations. Table 1 shows the nominal values, as well as the upper and lower boundaries, for various system variables gathered from the laboratory setting described in reference [5]. Besides, Figure 3 displays the nominal open-loop unit step response of the roll dynamical system (in the absence of control), proving that the system is innately unstable since the roll position grows with time unboundedly.

Table 1. Nominal, lower and upper bounds of the system variable [2–5]

Parameters	Lower Bounds	Nominal Values	Upper Bounds
d	0.18 m	0.2 m	0.22 m
C_l	0.324	0.36	0.396
J_x	0.01296 $\text{kg} \cdot \text{m}^2$	0.0144 $\text{kg} \cdot \text{m}^2$	0.01584 $\text{kg} \cdot \text{m}^2$

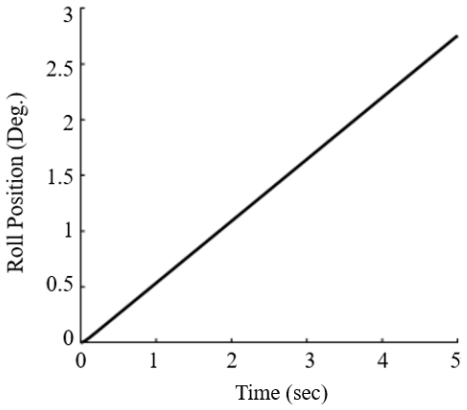

Figure 3. Nominal open-loop unit step response of the system

3 Controller Design

This section outlines the conceptual framework for developing the optimal robust deadbeat controller, which is used to control the roll-angle action of the tail-sitter VTOL UAV with the transfer function given in Eq. (7). In the beginning, it is crucial to identify the standards that the controller has to satisfy, which involve [4, 18, 19]:

(a) Retaining consistent robustness and efficiency in spite of changes in the model variables.

(b) Ability to disregard or attenuate disturbances.

(c) Practically feasible control exertion.

(d) Compliance with the set time response criteria.

The most important stage in the design process involves choosing the nominal representation of the system, followed by modelling the system uncertainty as a multiplicative model using the following formula [4]:

$$G_U(s) = G_n(s)\,(1 + \delta_m(s)) \tag{8}$$

where, $G_n(s)$ denotes the system nominal model based on nominal values mentioned in Table 1, and $\delta_m(s)$ indicates the multiplicative uncertainty model. The two functions are illustrated as follows:

$$G_n(s) = \frac{13.889}{s^2 + 25s} \tag{9}$$

$$\delta_m(s) = \frac{G_U(s) - G_n(s)}{G_n(s)} \tag{10}$$

In addition [4, 15]:

$$\delta_m(s) = W_m(s)\tilde{\delta}(s) \tag{11}$$

where, $W_m(s)$ is the uncertainty weighting function, and $\tilde{\delta}(s)$ refers to the continuous uncertainty variations with a magnitude of $|\tilde{\delta}(j\omega)| \leq 1$, with ω as the radian frequency variable.

Proposition 3: For improved robustness, the function $\delta_m(s)$ must be modelled in terms of the uncertainty worst-case issue. Therefore, $|\tilde{\delta}(j\omega)|$ is set to its largest value and $W_m(s)$ to equal the maximum limit of the uncertainty barrier $\rho(\omega)$ over all variants, i.e. [4, 15] :

$$|W_m(j\omega)| = |\delta_m(j\omega)| = \rho(\omega) \quad \forall\omega \tag{12}$$

In turn, based on Proposition 3 and Eq. (10), the uncertainty grading function is formed for every change in the system elements using MATLAB's curve fitting functionalities, providing the resultant uncertainty weight as:

$$W_m(s) = \frac{0.3829s + 195.1}{s + 1200} \tag{13}$$

On another point, for more robust efficiency despite disturbances, an effective robust performance weighting function is used as follows [4, 15]:

$$W_p(s) = \frac{\frac{1}{M_s}s + \omega_B}{s + \omega_B e_{ss}} \tag{14}$$

where, the bandwidth ω_B, peak amplitude M_S, and stability error e_{ss} are crucial factors in ensuring robustness and preventing disruptive high-frequency perturbations, with M_S less than 2 .

The planned control's thorough investigation is specified by means of the sensitivity function $S(s)$ and the associated closed-loop function $C(s)$, whereby [4, 18, 19]:

$$\begin{cases} S(s) = \frac{1}{1+G_n G_{DB}(s)} \\ C(s) = \frac{G_n G_{DB}(s)}{1+G_n G_{DB}(s)} \end{cases} \tag{15}$$

where, $G_{DB}(s)$ refers to the proposed deadbeat controller that is defined with two components. The main component is the inverse of the nominal model of the system $G_n(s)$ that eliminates the instability dynamics through feedback multiplied by the deadbeat response component employed for imposing the intended response attributes as follows [15, 20]:

$$G_{DB}(s) = \frac{1}{G_n(s)}\left(\frac{T(s)}{1-T(s)}\right) \tag{16}$$

where, $T(s)$ refers to the deadbeat response component of the controller function. In this study, $T(s)$ is selected in the form such that:

$$\frac{T(s)}{1-T(s)} = \frac{\omega_n^2}{s^2 + 2\zeta\omega_n s + \omega_n^2} \tag{17}$$

In this case, the required time response features are governed by the values of the natural frequency ω_n in *rad/sec* and the damping ratio ζ.

Proposition 4: To broaden the generality of the proposed control technique to other systems, the deadbeat part of the controller should be chosen so that the transfer function $G_n G_{DB}(s)$ is strictly proper, or at least proper, ensuring the stability of the applied controller. As a result, the boundedness of the closed-loop signals. Table 2 outlines the fundamental usable functions for the controller's deadbeat component and the type of system they could be employed for, as well as the response variables that are controlled for each component.

Table 2. Basic forms of the controller deadbeat component

$\frac{\mathbf{T(s)}}{\mathbf{1-T(s)}}$	**Controlled System Order**	**Response Control Variables**
$\frac{K_c}{\tau s+1}$	First	The gain K_c and time constant τ
$\frac{\omega_n^2}{s^2+2\zeta\omega_n s+\omega_n^2}$	First and second	The natural frequency ω_n and damping ratio ζ
$\frac{\omega_n^3}{s^3+1.75\omega_n s^2+2.15\omega_n^2 s+\omega_n^3}$	First, second, and third	The natural frequency ω_n

The final phase of the controller design problem is the efficient determination of the controller settings ω_n and ζ to provide the control system with powerful stability and performance, together with the parameters ω_B, M_S, and e_{ss} such that the following robustness condition in terms of the H_∞ concept is satisfied [4, 18, 19]:

$$\begin{aligned} &\left\| \begin{matrix} W_p S(j\omega) \\ W_m C(j\omega) \end{matrix} \right\|_\infty \leq 1 \quad \forall\omega \Rightarrow \\ &\|W_p S(j\omega)\|_\infty + \|W_m C(j\omega)\|_\infty \leq \|W_p S(j\omega) + W_m C(j\omega)\|_\infty \leq 1 \quad \forall\omega \end{aligned} \tag{18}$$

Or:

$$\begin{cases} S(j\omega) \leq \frac{1}{W_p(j\omega)} \\ C(j\omega) \leq \frac{1}{W_m(j\omega)} \end{cases} \quad \forall\omega \tag{19}$$

where, $\|.\|_\infty$ represents the H_∞ norm mapping operator. To accomplish this goal, the IbILO algorithm is employed as an extremely useful strategy, which is separated into numerous phases given below. All phases serve a specific purpose. Whenever a particular step finishes, the findings go on to the next phase, without returning to the present iteration [16, 17]. This study employs the IbILO method, utilizing the optimization settings outlined in Table 3 , to reduce the fitness function to less than 1 .

$$F\left(\omega_n, \zeta, \omega_B, M_S, e_{ss}\right) = \left\|W_p s(j\omega) + W_m c(j\omega)\right\|_\infty \tag{20}$$

Table 3. Optimization settings of the IbILO algorithm

Optimization Setting	Value
Number of experts (population)	50
Number of optimized variables	5
Number of iterations	50
Number of initial phase models	5
Maximum percentage of iteration for the first phase	0.33
Maximum percentage of iteration for the second phase	0.33
Minimum value of the boundary	0.4
Maximum value of the boundary	0.6
Number of iteration classifications	100

4 Results

This section describes the simulation findings relating to implementing the proposed controller with the functions defined in Eq. (16) and Eq. (17) to the modelled system function of Eq. (7). To assess the nominal effectiveness characteristics, the results are first reported in the context of nominal ratings without the impact of uncertainty or atmospheric disturbance. The controller's robustness is then evaluated in spite of all perturbations, taking into account an exogenous disturbance of $d_w(t) = [-10°, 10°]$. For all findings, the reference roll angle position is $\phi_{\text{ref}}(t) = 30°$.

Table 4 initially presents the optimization outputs, demonstrating that the optimization method successfully identified the optimized values and produced a best cost value smaller than one, as illustrated in Figure 4, which satisfied the robustness rule defined by Eq. (18). The strength of the IBILO method can be manifested in attaining adequate controller gains with precisely set values of ω_B, M_S, and e_{ss}. This leads to reaching the minimum possible cost with sufficient fulfillment of time response criteria, mainly indicated by ω_n and ζ.

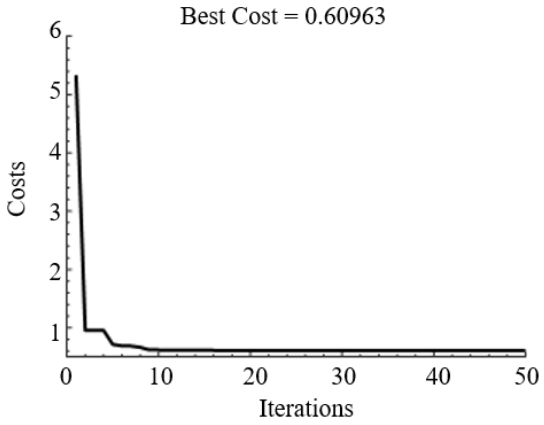

Figure 4. Cost function minimization over iterations

Table 4. Optimization results

Control System Variable	Value
ω_n	30
ζ	0.9
ω_B	0
M_S	1.8
e_{ss}	0.0067
Best cost	0.60963

Figure 5 displays the nominal roll position response of the control system, illustrating how stability was successfully raised with interest in rapidity and diminished overshoot. In addition, the conductance of the error signal in getting to zero is shown in Figure 6, confirming the envisioned tracking to the benchmark instruction.

The exercised control thrust input in Newton (*N*) is depicted in Figure 7, where it can be evident that the amount of control thrust provided to the UAV's body center is reasonable and realistic. Additionally, Figure 8 portrays the control system's unit ramp response, which shows that the steady-state response qualities are attained with a minimal error deviation between the roll position output and a continually increasing baseline input.

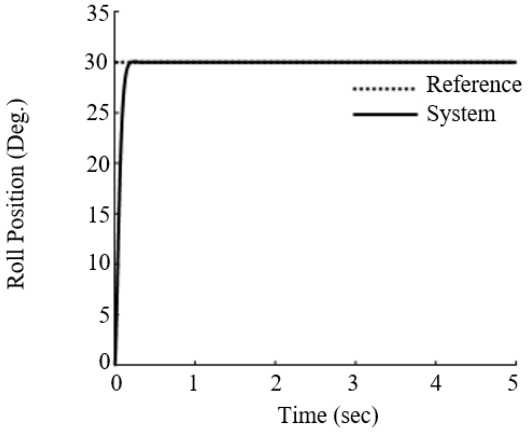

Figure 5. Nominal response of the controlled roll position

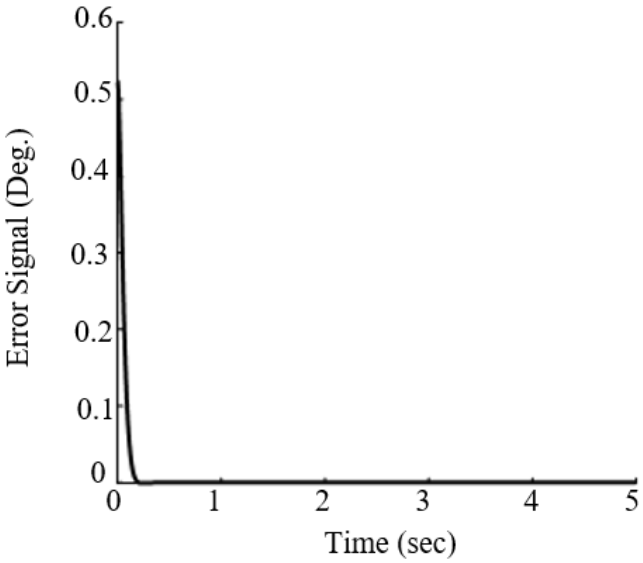

Figure 6. Action of the system error signal

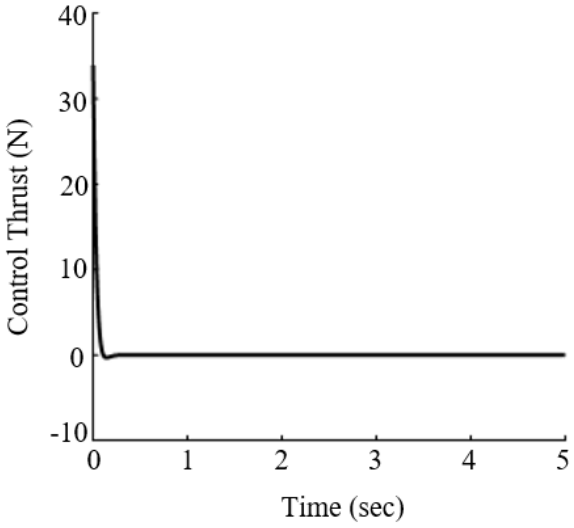

Figure 7. The exercised control thrust input

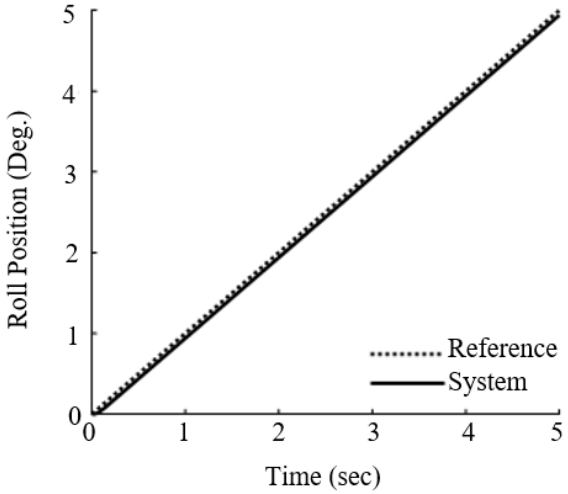

Figure 8. Unit ramp response of the controlled system

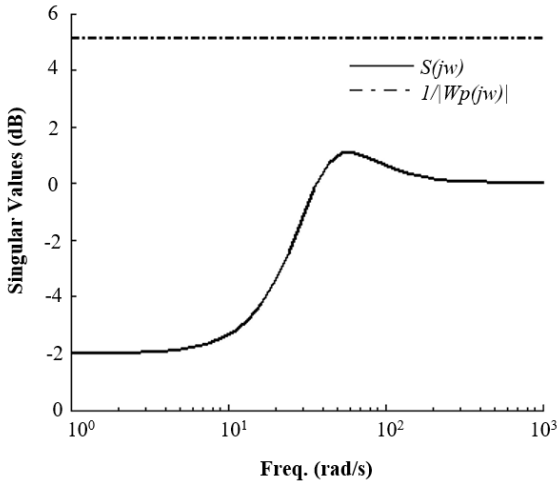

Figure 9. Magnitude plots of $S(s)$ versus $W_p(s)$

Concerning the robustness challenge in Eq. (18), Figure 9 and Figure 10 show that the proposed control is robust against systemic perturbations, as the magnitudes of the inverses of $W_p(s)$ and $W_m(s)$ are greater than the magnitudes of $S(s)$ and $C(s)$.

Finally, Figure 11 shows the reaction of the roll angle movement against overall uncertainty and disturbance, revealing that the controller has properly dealt with the system parametric uncertainty while tackling the adverse impact of wind disturbances with consistent and adequate error and control thrust behaviors, as evident in Figure 12.

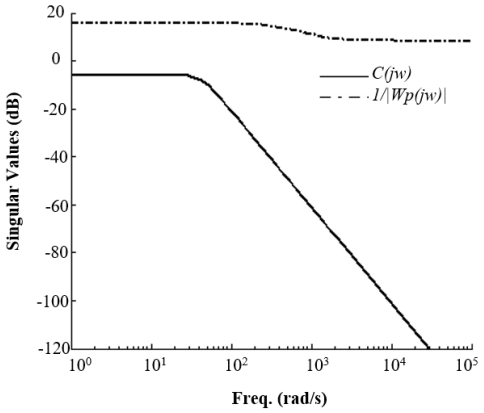

Figure 10. Magnitude plots of $C(s)$ versus $W_m(s)$

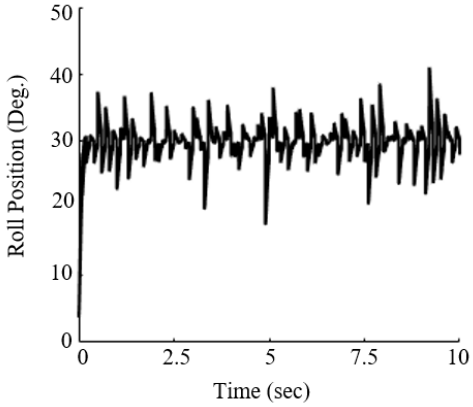

Figure 11. Uncertain response of the controlled roll position

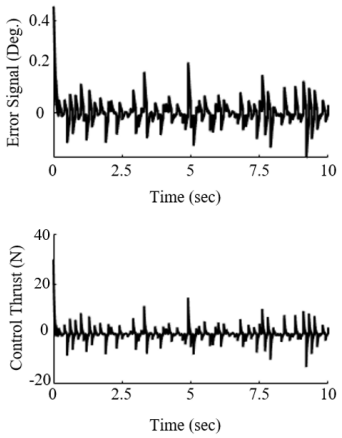

Figure 12. Uncertain behaviors of the error and control signals

The current study presents a more effective and easier approach to regulating VTOL aircraft control than previous research. It offers a simpler controller layout than MRAC [3], reducing development complications and calibration attempts. The proposed technique improves deadbeat control for tail-sitter UAV behavior, outperforming MRAC with dead-zone modification in overall control effectiveness. This approach is more effective and easier to implement than previous methods, such as Grey Wolf Optimization (GWO) [2], which may struggle with changing dynamics. Additionally, the proposed method has been compared to control methods in some studies [4, 5], demonstrating several advantages over previous works, as illustrated in Table 5. The promoted control scheme beats earlier efforts in terms of accurate positioning of the roll angle with a small overshoot rate. It yields a robust process with desirable response rapidity, as indicated by short rise and settling periods. For such insecure processes, this approach ensures accurate motion and a speedy arrival at the needed tasks.

Table 5. Comparison of the suggested control to earlier-posed strategies [4, 5]

Performance Criterion	Proposed Controller	Controller of the Study [4]	Controller of the Study [5]
Rise time (sec)	0.0965	0.0398	0.125
Settling time (sec)	0.1134	0.12	2.1
Overshoot (%)	0.167	3.32	23

5 Conclusions

This study describes the development of a robust deadbeat controller for the roll attitude of a tail-sitter VTOL UAV. Initially, a model-building method was implemented to acquire a sufficient mathematical model by considering the system parameter fluctuations as well as the exogenous wind effect. To solve the system difficulties, the controller was designed considering the known features of the system and robustness standards. Then the development procedure was refined by applying the IbILO algorithm. Ultimately, the controller's functionality was examined, and the numerical simulation outcomes demonstrated enhanced stability and efficiency, providing several advantages beyond existing control approaches. The major drawback of this strategy lies in its linearity regulation, so it may lack confidence in its efficacy towards more complicated disruptions, such as operating in elevated frequency areas that are far from the guaranteed stability conditions. Prospective studies may employ the wide variety of concepts acquired from the entire design to apply the proposed controller to further systems by determining the system's deadbeat action, creating an accurate system model, and distinguishing the categories of perturbations to be handled by the control technique.

Data Availability

The data used to support the research findings are available from the corresponding author upon request.

Conflicts of Interest

The authors declare no conflict of interest.

References

[1] A. S. Saeed, A. B. Younes, C. X. Cai, and G. W. Cai, "A survey of hybrid unmanned aerial vehicles," *Prog. Aerosp. Sci.*, vol. 98, pp. 91–105, 2018. https://doi.org/10.1016/j.paerosci.2018.03.007

[2] A. A. Al-Qassar, A. I. Abdulkareem, A. F. Hasan, A. J. Humaidi, I. K. Ibraheem, A. T. Azar, and A. H. Hameed, "Grey-wolf optimization better enhances the dynamic performance of roll motion for tail-sitter VTOL aircraft guided and controlled by STSMC," *J. Eng. Sci. Technol.*, vol. 16, no. 3, pp. 1932–1950, 2021.

[3] A. R. Ajel, A. J. Humaidi, I. K. Ibraheem, and A. T. Azar, "Robust model reference adaptive control for tail-sitter VTOL aircraft," *Actuators*, vol. 10, no. 7, p. 162, 2021. https://doi.org/10.3390/act10070162

[4] A. H. Mhmood and H. I. Ali, "Optimal H-infinity PID model reference controller design for roll control of a tail-sitter VTOL UAV," *Eng. Technol. J.*, vol. 39, no. 4A, pp. 552–564, 2021. https://doi.org/10.30684/etj.v39 i4A.1861

[5] H. Abrougui, S. Nejim, and H. Dallagi, "Roll control of a tail-sitter VTOL UAV," *Int. J. Control. Energy. Electr. Eng.*, vol. 7, pp. 22–27, 2019.

[6] W. F. Wang, J. H. Zhu, M. C. Kuang, X. M. Yuan, Y. F. Tang, Y. Q. Lai, L. J. Chen, and Y. J. Yang, "Design and hovering control of a twin rotor tail-sitter UAV," *Sci. China Inf. Sci.*, vol. 62, no. 9, p. 194202, 2019. https://doi.org/10.1007/s11432-018-9733-8

[7] S. Garcia-Nieto, J. Velasco-Carrau, F. Paredes-Valles, J. V. Salcedo, and R. Simarro, "Motion equations and attitude control in the vertical flight of a VTOL bi-rotor UAV," *Electronics*, vol. 8, no. 2, p. 208, 2019.

[8] J. M. O. Barth, J. P. Condomines, M. Bronz, J. M. Moschetta, C. Join, and M. Fliess, "Model-free control algorithms for micro air vehicles with transitioning flight capabilities," *Int. J. Micro Air Veh.*, vol. 12, p. 1756829320914264, 2020. https://doi.org/10.1177/1756829320914264

[9] W. F. Zhou, S. Y. Chen, C. W. Chang, C. Y. Wen, C. K. Chen, and B. Y. Li, "System identification and control for a tail-sitter unmanned aerial vehicle in the cruise flight," *IEEE Access*, vol. 8, pp. 218 348–218 359, 2020. https://doi.org/10.1109/ACCESS.2020.3042316

[10] H. B. Xin, Y. J. Wang, X. Z. Gao, Q. Y. Chen, B. J. Zhu, J. F. Wang, and Z. X. Hou, "Modeling and control of a quadrotor tail-sitter unmanned aerial vehicle," *Proc. Inst. Mech. Eng. Part I J. Syst. Control Eng.*, vol. 236, no. 3, pp. 443–457, 2022. https://doi.org/10.1177/09596518211050466

[11] E. Tal and S. Karaman, "Global incremental flight control for agile maneuvering of a tailsitter flying wing," *J. Guid. Control Dyn.*, vol. 45, no. 12, pp. 2332–2349, 2022. https://doi.org/10.2514/1.G006645

[12] J. Y. Zhong, C. Wang, and H. Zhang, "Transition control of a tail-sitter unmanned aerial vehicle with L1 neural network adaptive control," *Chin. J. Aeronaut.*, vol. 36, no. 7, pp. 460–475, 2023. https://doi.org/10.1016/j.cja.2023.04.002

[13] Y. J. Yang, J. H. Zhu, X. M. Yuan, X. Y. Wang, M. C. Kuang, and H. Shi, "Dynamic characteristics analysis and robust transition control of tail-sitter VTOL UAVs," *Aerosp. Sci. Technol.*, vol. 145, p. 108868, 2024. https://doi.org/10.1016/j.ast.2024.108868

[14] R. C. Dorf and R. H. Bishop, *Modern Control Systems*. New Jersey: Pearson Education, 2016.

[15] H. I. Ali, "Robust deadbeat controller design using PSO for positioning a permanent magnet stepper motors," *Iraqi J. Comput. Commun. Control Syst. Eng.*, vol. 12, no. 1, pp. 32–41, 2012.

[16] M. Mirrashid and H. Naderpour, "Incomprehensible but intelligible-in-time logics: Theory and optimization algorithm," *Knowl.-Based Syst.*, vol. 264, p. 110305, 2023. https://doi.org/10.1016/j.knosys.2023.110305

[17] F. A. Samoon, I. Hussain, and S. J. Iqbal, "ILA optimisation based control for enhancing DC link voltage with seamless and adaptive VSC control in a PV-BES based AC microgrid," *Energies*, vol. 16, no. 21, p. 7309, 2023. https://doi.org/10.3390/en16217309

[18] M. K. Yang, Y. L. Li, H. Du, C. Li, and Z. Y. He, "Hierarchical multiobjective H-infinity robust control design for wireless power transfer system using genetic algorithm," *IEEE Trans. Control Syst. Technol.*, vol. 27, no. 4, pp. 1753–1761, 2019. https://doi.org/10.1109/TCST.2018.2814589

[19] X. Yan, P. F. Wang, J. Y. Qing, S. F. Wu, and F. Y. Zhao, "Robust power control design for a small pressurized water reactor using an H infinity mixed sensitivity method," *Nucl. Eng. Technol.*, vol. 52, no. 7, pp. 1443–1451, 2020. https://doi.org/10.1016/j.net.2019.12.031

[20] G. Elhassan, S. A. Zulkifli, S. Z. Iliya, H. Bevrani, M. Kabir, R. Jackson, M. H. Khan, and M. Ahmed, "Deadbeat current control in grid-connected inverters: A comprehensive discussion," *IEEE Access*, vol. 10, pp. 3990–4014, 2022. https://doi.org/10.1109/ACCESS.2021.3138789